

Heat conduction in a solid slab embedded with a pipe of general cross section: Shape Factor and Shape Optimization

Marios M. Fyrillas*
Department of Mechanical Engineering
Frederick University Cyprus, 1303 Nicosia, Cyprus

October 23, 2008

Abstract

We address the problem of two-dimensional heat conduction in a solid slab embedded with an isothermal, symmetric pipe of general cross section. Similar formulations have applications in continuum mechanics and electricity. The main objective of this work is to develop a Shape Optimization algorithm that will reveal the optimal shapes of the pipe such that the conduction rate is maximized or minimized. This is achieved by optimizing the Shape Factor. To obtain the Shape Factor we transform the pipe into a strip using the generalized Schwarz-Christoffel transformation, and develop an integral equation of the first kind for the temperature gradient using Fourier transform techniques. The integral equation is solved both numerically and analytically/asymptotically. The fact that the Shape Factor is a monotonic function of the length of the strip suggests a Shape Optimization formulation where the objective function is the length of the strip and the variables of the optimization are the parameters of the generalized Schwarz-Christoffel transformation. Optimal shapes for the problem of minimizing the conduction rate are computed numerically and validated with an analytical solution. Numerical results for maximizing the transport rate are also obtained. The versatility and the robustness of the numerical optimization algorithm offers opportunities for improving the design of similar processes with non-linear equality and inequality constraints.

Keywords

Shape Optimization; Shape Factor; generalized Schwarz-Christoffel transformation; Laplace equation; two-dimensional heat conduction; solid slab.

1 Introduction

The problem of heat conduction in a solid slab embedded with an isothermal pipe is of fundamental importance in many engineering applications [17]: i) heat conduction in a solid slab impregnated with a heating pipe, ii) heat conduction due to a transistor embedded in

*E-mail: m.fyrillas@frederick.ac.cy

a large silicon substrate [17] and iii) temperature distribution in floor heating systems [7]. In addition, similar formulations have applications in continuum mechanics, electricity and heat conduction [23, 27, 25].

The main contribution of this work is to develop a numerical Shape Optimization algorithm which would reveal the optimal shapes of the pipe such that the conduction rate is maximized or minimized. This is achieved by optimizing the Shape Factor. While the formulation and solution of the heat conduction problem is standard and in this sense the paper does not extend one's knowledge of engineering science, the formulation of the Shape Optimization problem is new and offers new and significant findings. More important, we believe that it can be easily extended to include linear, non-linear equality and/or inequality constraints. From an engineering perspective, knowledge of a surface geometry that maximizes or minimizes the transport rate offers opportunities for improving the design of a broad range of engineering processes and products. General considerations of optimal shape design can be found in Pironneau [26] and Bejan [2]. Applications include drag reduction in external flows [5], the design of minimum seepage loss canals [18, 30], and the minimization of the thermal resistance of an inverted fin [3] intruding into a conducting wall. An example from electricity that is closely related to the present work, and in particular to the conduction minimization problem, is the two-dimensional potential problem for a finite plate charged to an arbitrary potential situated between parallel earthed planes [23, 19]. In fact there is excellent agreement between the analytical and numerical results (Section §4.1).

The problem we address in this work is that of heat conduction in a slab of finite thickness embedded with an isothermal, symmetric pipe of general cross section. The upper and lower surfaces of the slab are kept at a constant temperature and the pipe is at the midsection of the slab. Using conformal mapping techniques [4], and in particular the generalized Schwarz-Christoffel transformation [8, 6], we transform the problem to that of heat conduction due to an isothermal strip placed at the midsection of the slab. In view of the conformal transformation, the Shape Factor of the pipe and its associated strip are equal [4]. The Shape Factor of the strip can be obtained through different techniques [15, 27]. Given the complexity of these results, we develop a Fredholm integral equation of the first kind for the temperature gradient along the strip using Fourier transform techniques. The integral equation can be easily addressed both asymptotically and numerically as outlined in [13] and [29].

The fact that the Shape Factor is a monotonic function of the length of the strip suggests a Shape Optimization procedure where the objective function is the length of the strip and the variables of the optimization are the parameters of the generalized Schwarz-Christoffel transformation. It is a nonlinear programming problem (constrained nonlinear optimization [11, 22]). The objective is to find the constrained maximum/minimum of a scalar function of several variables. The Shape Optimization problem is addressed through numerical optimization which can handle complicated geometrical constraints. The robustness and the versatility of the formulation offers opportunities for improving the design of a broad range of engineering processes and products.

In the next Section (§2) we develop a conformal mapping technique where a symmetric isothermal pipe, embedded at the midsection of a slab, is mapped into a finite strip.

In Section (§3) we address, both analytically (asymptotically) and numerically, the two-dimensional, heat conduction problem in slab embedded with an isothermal, finite strip. In Section (§4) we pose and solve numerically two Shape Optimization problems. Our objective is twofold: i) given the surface area of the pipe to find the shape that maximizes the transport rate and ii) given the volume of the pipe to find the shape that minimizes the transport rate. The former is associated with maximizing the transport rate given the perimeter length of the cross-sectional profile while the latter is associated with maximizing the transport rate given the cross-sectional area. We summarize our findings in the last Section.

2 Conformal transformation of the pipe into a strip

In this section we consider heat conduction due to an isothermal (T_1) symmetric pipe of general cross section, embedded at the center of a solid slab. The upper and lower surfaces of the slab are maintained at temperature T_2 as shown in Figure (1). In what follows we non-dimensionalize the lengths with the height H , and the temperature field by subtracting T_2 and dividing by the temperature difference $T_1 - T_2$. Without loss of generality we assume that the left point of symmetry of the pipe coincides with the origin of the coordinate system. Finding the Shape Factor of such a pipe relies on finding a conformal transformation that transforms the pipe into a strip. For a general shape this can be achieved by discretizing the boundary of the pipe into straight segments. Then, using the generalized Schwarz-Christoffel transformation, the upper-half of the pipe is transformed into a strip. We consider only the upper half in view of the symmetry of the problem. The formulation is also relevant for an isothermal object embedded in a large, non-conducting substrate. We outline the procedure in what follows.

As described by Davis [6] and Floryan [12] an arbitrary channel, bounded by polygonal segments in the physical domain, can be mapped into a straight channel in the computational domain using the generalized Schwarz-Christoffel transformation (Figure 2)

$$\frac{dz}{dw} = R \prod_{j=0}^{j=N} \left[\sinh \frac{\pi}{2h} (w - w_j) \right]^{\alpha_j}, \quad (1)$$

where the product identifies the number of elements (N). In the above transformation w_j are the images of the z_j vertices (Figure 2), $\pi\alpha_j$ are the turning angles which are taken to be positive for the clockwise rotation, α_0 and α_N are defined with respect to the x -axis, and R is a complex constant. For the configurations we will be considering, the x -axis is the boundary at $\pm\infty$ hence R is a real number and

$$\sum_j \alpha_j = 0. \quad (2)$$

The transformation is defined uniquely by placing the origin of the transformed domain at the origin of the physical domain and by choosing an arbitrary point [12]. This choice is

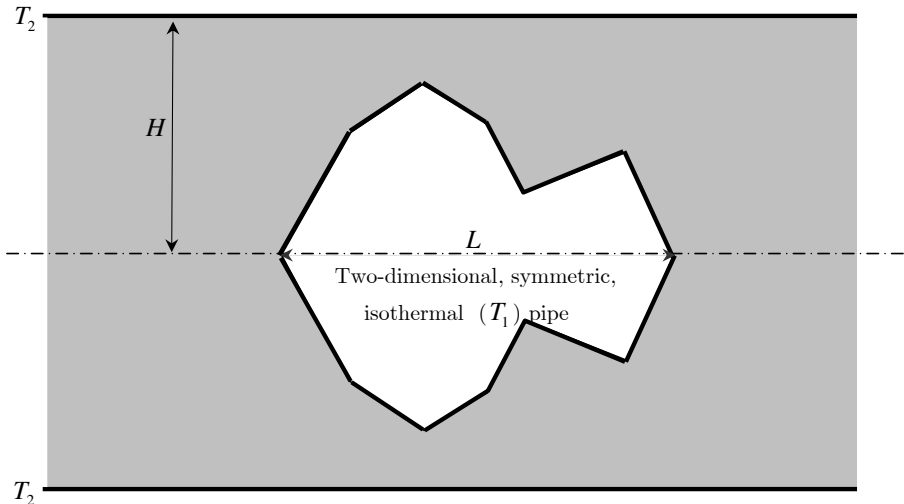


Figure 1: Schematic representation of the physical problem. The surfaces of the slab are kept at a constant temperature T_2 and the distance between them is $2H$. At the mid-distance there is a two-dimensional isothermal symmetric pipe of general cross section and length L which is kept at temperature T_1 .

accomplished by placing the first bottom corner at the origin of the w -plane ($w_0 = 0$). In view of these choices and upon integration the transformation takes the form

$$z(w; \boldsymbol{\alpha}) = R \int_0^w \prod_{j=0}^{j=N} \left[\sinh \frac{\pi}{2h} (\theta - w_j) \right]^{\alpha_j} d\theta, \quad (3)$$

where $\boldsymbol{\alpha}$ represents the $N+1$ -tuple $(\alpha_0, \alpha_1, \alpha_2, \dots, \alpha_N)$. The constant R is fixed by stipulating that the upper wall of the physical plane, i.e. the line $z = i$, transforms to $w = i$, i.e. $h = 1$:

$$R = \frac{1}{\text{Im}[z(i; \boldsymbol{\alpha})]}. \quad (4)$$

The parameters (w_j and R with the exception of w_0) of the transformation (3) do not appear explicitly but given the physical domain, and hence the angles $\pi\alpha_j$, a system of non-linear equations must be solved for the unknown parameters [8]. Alternatively, Davis [6] also suggested that these constants can be efficiently determined through a method of successive approximations [12]. Once the value of w_N has been calculated, the Shape Factor of the pipe is simply the Shape Factor of a strip of length w_N which can be obtained through the results of the next Section (§3). This simple result is due to the conformal transformation; the Shape Factor of the pipe and its associated strip are equal.

Here, we should point out that the optimization problem that we will address in Section (§4) is an inverse problem. Whereas the classical approach is to compute the w_j s and R (with the exception of w_0), in the Shape Optimization we need to compute the α_j s and R while the w_j s can be defined a priori without loss of generality.

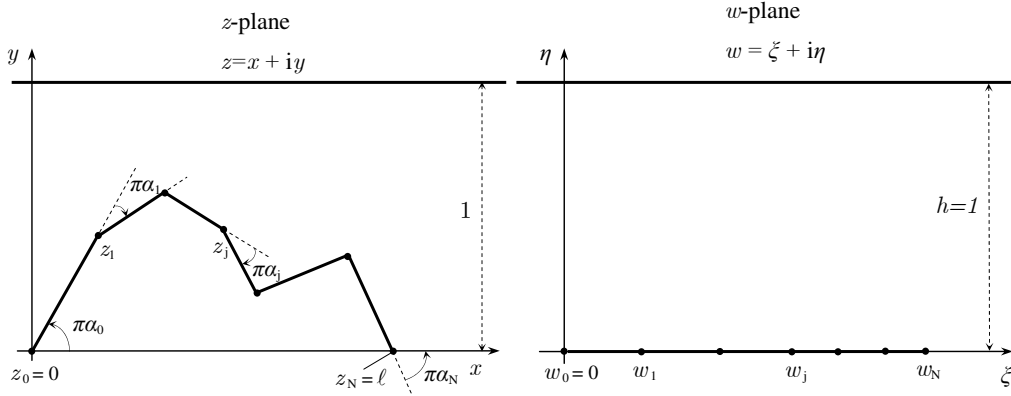


Figure 2: Mapping of the upper half of the pipe in the physical plane into a strip in the transformed domain. The lengths have been non-dimensionalized with the height H , i.e. $\ell = L/H$.

3 Heat conduction due to an isothermal strip

The basic problem associated with our analysis is that of heat conduction in a slab where the upper and lower surfaces are kept at a constant temperature $T = 0$. At the center of the slab there is a two-dimensional (infinite span) isothermal strip of length w_N which is kept at temperature $T = 1$. In view of the symmetry of the problem, the boundary conditions are as follows:

$$\begin{aligned} \text{On } \eta = 0 & \begin{cases} \frac{\partial T}{\partial \eta} = 0 & \text{for } \xi > w_N \text{ and } \xi < 0 \\ T = 1 & \text{on } 0 \leq \xi \leq w_N \end{cases}, \text{ and} \\ \text{On } \eta = 1 & T = 0. \end{aligned} \quad (5)$$

The mathematical model along with the boundary conditions are shown in Figure (3).

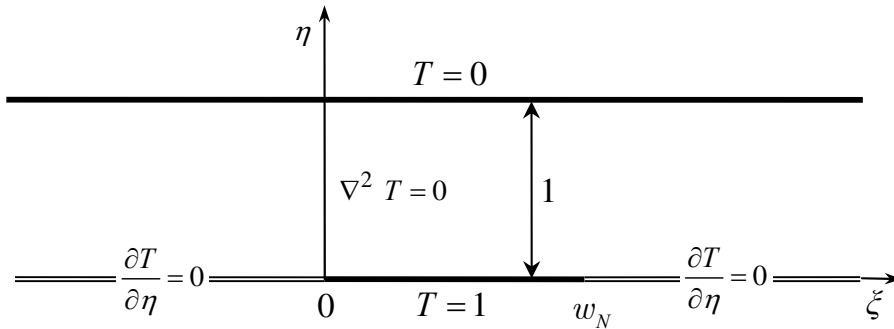


Figure 3: Schematic representation of the model problem along with boundary conditions. The Neumann boundary is dictated by the symmetry of the pipe.

In the next section we obtain a Fredholm integral equation of the first kind for the

temperature gradient along the strip which is solved numerically. In addition we obtain asymptotic results for both small and large w_N .

3.1 Shape Factor

The strip problem was originally addressed by Hahne [15] and Ranger [27] using conformal mapping and Green's function techniques. In this work we employ Fourier Transform techniques which prove to be less tedious and more general as they can be applied to problems with more general boundary conditions [28, 16]. We obtain a Fredholm integral equation of the first kind for the temperature gradient along the strip, i.e. $\frac{\partial T(\eta=0)}{\partial \eta}$ on $0 \leq \xi \leq w_N$, which we solve both analytically/asymptotically and numerically. The Shape Factor (S) [17] associated with a strip of span z is equal to

$$S = -z w_N \int_0^1 \frac{\partial T(\hat{\xi}, \eta = 0)}{\partial \eta} d\hat{\xi}, \quad (6)$$

where $\hat{\xi} = \xi/w_N$.

3.1.1 Analysis

We denote the Fourier Transform of a function $f(\xi)$ as $\mathcal{F}(f) \equiv \tilde{f}(\mathbf{w})$ [20]. We apply the Fourier Transform on the Laplace equation in the ξ -direction to obtain:

$$\frac{d^2 \tilde{T}(\mathbf{w}, \eta)}{d\eta^2} - \mathbf{w}^2 \tilde{T}(\mathbf{w}, \eta) = 0.$$

The solution that satisfies the boundary condition at $\eta = 1$ (equation 5) is

$$\tilde{T}(\mathbf{w}, \eta) = A(\mathbf{w}) \sinh[\mathbf{w}(\eta - 1)]. \quad (7)$$

The constant $A(\mathbf{w})$ can be expressed in terms of the Fourier Transform of the temperature gradient on $\eta = 0$ as

$$A(\mathbf{w}) = \frac{\partial \tilde{T}(\mathbf{w}, \eta = 0)}{\mathbf{w} \cosh \mathbf{w}}.$$

Substituting above equation in equation (7) and evaluating at $\eta = 0$ we obtain the Fourier Transform of the temperature at the lower boundary:

$$\tilde{T}(\mathbf{w}, \eta = 0) = -\frac{\partial \tilde{T}(\mathbf{w}, \eta = 0)}{\partial \eta} \frac{\tanh \mathbf{w}}{\mathbf{w}}.$$

Taking the inverse Fourier Transform of above expression, employing the convolution theorem and that $\mathcal{F}^{-1}(\tanh \mathbf{w}/\mathbf{w}) = \sqrt{2/\pi} \ln [\coth(\pi|\xi|/4)]$ (see appendix A; equation 21) the temperature at the lower wall becomes:

$$T(\xi, \eta = 0) = -\frac{1}{\pi} \int_{-\infty}^{\infty} \frac{\partial T(\theta, \eta = 0)}{\partial \eta} \ln \left[\coth \left(\frac{1}{4} \pi |\xi - \theta| \right) \right] d\theta.$$

Employing the boundary condition at $\eta = 0$ (Equation 5) and normalizing ξ and θ with w_N , i.e. $\hat{\theta} = \theta/w_N$, above equation leads to a Fredholm integral equation of the first kind for the temperature gradient along the strip

$$1 = -\frac{w_N}{\pi} \int_0^1 \frac{\partial T(\hat{\theta}, \eta = 0)}{\partial \eta} \ln \left[\coth \left(\frac{1}{4} \pi w_N |\hat{\xi} - \hat{\theta}| \right) \right] d\hat{\theta}. \quad (8)$$

3.1.2 Results

For small w_N , the integral equation (8) simplifies to

$$1 = -\frac{w_N}{\pi} \int_0^1 \frac{\partial T(\hat{\theta}, \eta = 0)}{\partial \eta} \ln \left[\left(\frac{1}{4} \pi w_N |\hat{\xi} - \hat{\theta}| \right)^{-1} \right] d\hat{\theta}.$$

In view of identity (20) (see appendix A) we assume a solution of the form

$$\frac{\partial T(\hat{\theta}, \eta = 0)}{\partial \eta} = \frac{a_0}{\sqrt{\hat{\theta}(1 - \hat{\theta})}},$$

which reduces the integral equation to an algebraic equation [13] with solution

$$a_0 = \frac{1}{w_N \ln(\pi w_N / 16)}.$$

Hence, for small values of w_N , the Shape Factor is equal to

$$S(w_N \ll 1) = -\frac{z \pi}{\ln(\pi w_N / 16)}, \quad (9)$$

while for large values of w_N , wherein the problem is that of heat conduction between two parallel plates, the Shape Factor is

$$S(w_N \gg 1) = z w_N. \quad (10)$$

Results (9) and (10) agree with the asymptotic results given in [15].

The numerical method used is the collocation boundary element method, where the local basis functions are step functions, i.e. the boundary ($0 \leq \hat{\xi} \leq 1$) is discretized into segments (boundary elements), and it is assumed that the unknown function is constant over each element. As shown in Figure (4), there is excellent agreement between the asymptotic results (9, 10) and the numerical solution.

In the next section, based on the findings of the preceding sections, we pose a Shape Optimization problem associated with maximizing or minimizing the transport rate from a two-dimensional pipe of unit span.

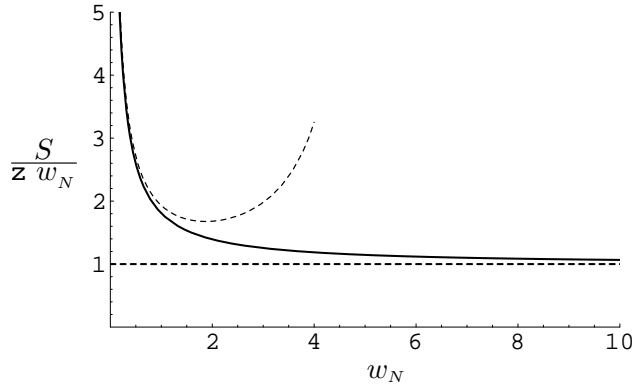


Figure 4: Computed values of the Shape Factor. The solid curve corresponds to numerical results and the dashed curves to asymptotic results. The thin-dashed curve corresponds to equation (9) (small w_N) while the thick dashed line to equation (10) (large w_N).

4 Shape Optimization

Based on the findings of the previous Sections (§2 and §3), we can conclude that:

- The Shape Factor of a two dimensional, isothermal symmetric pipe embedded at the center of a solid slab can be found by transforming the half-pipe into a strip of length w_N (Section §3) using the generalized Schwarz-Christoffel transformation. The Shape Factor of the pipe is equal to the Shape Factor of the strip.
- The Shape Factor of an isothermal strip embedded at the center of a solid slab is a monotonic function of its length (w_N), i.e. the longer the strip the higher the transport rate (Section §2).

Hence, given a number of pipe-shapes, the one responsible for the higher transport rate is the one associated with the larger value of w_N while the one responsible for the smaller transport rate is the one associated with the smaller value of w_N . *Therefore, the objective function of the optimization procedure is w_N .*

In what follows, we pose two Shape Optimization problems. Our objective is twofold: i) given the surface area of the pipe to find the shape that maximizes the transport rate and ii) given the volume of the pipe to find the shape that minimizes the transport rate. For a pipe of unit span, the former is associated with maximizing the transport rate given the perimeter length of the cross-sectional profile while the latter is associated with maximizing the transport rate given the cross-sectional area.

For reasons that will be apparent subsequently we normalize z , w and θ in equation (3) with respect to w_N

$$\hat{z}(\hat{w}; \alpha, w_N) = R \int_0^{\hat{w}} \prod_{j=0}^{j=N} \left[\sinh \frac{w_N \pi}{2} (\hat{\theta} - \hat{w}_j) \right]^{\alpha_j} d\hat{\theta},$$

and we define

$$\hat{z}_i = \hat{z}_i(\boldsymbol{\alpha}, w_N) = \hat{z}(\hat{w}_i; \boldsymbol{\alpha}, w_N) = R \int_0^{\hat{w}_i} \prod_{j=0}^{j=N} \left[\sinh \frac{w_N \pi}{2} (\hat{\theta} - \hat{w}_j) \right]^{\alpha_j} d\hat{\theta}, \quad (11)$$

where, as mentioned earlier, the \hat{w}_i s (and \hat{w}_j s) are preassigned; for example equispaced points ($N+1$ -tuple) between 0 and 1.

In what follows we develop an optimization strategy in order to maximize/minimize w_N subject to certain geometrical constraints, i.e. the perimeter length and the cross-sectional area of the half-pipe (upper half). We define the dimensionless length of the polygonal segments associated with the half-pipe

$$P(\boldsymbol{\alpha}) = w_N \sum_{j=0}^{N-1} |\hat{z}_{j+1} - \hat{z}_j|, \quad (12)$$

and the dimensionless area associated with the cross sectional area of the half-pipe

$$A(\boldsymbol{\alpha}) = w_N^2 \sum_{j=0}^{N-1} \frac{\text{Im}(\hat{z}_{j+1} + \hat{z}_j)}{2} \text{Re}(\hat{z}_{j+1} - \hat{z}_j) = \frac{w_N^2}{2} \sum_{j=0}^{N-1} (\hat{y}_{j+1} + \hat{y}_j)(\hat{x}_{j+1} - \hat{x}_j). \quad (13)$$

We proceed to formulate the optimization problems with respect to w_N as justified. Maximizing the transport rate, given the perimeter length of the cross-sectional profile of the pipe, is equivalent to maximizing w_N . In view of equation (12) the problem is formulated as follows:

$$\underset{\boldsymbol{\alpha}}{\text{minimize}} \quad \sum_{j=0}^{N-1} |\hat{z}_{j+1} - \hat{z}_j| \quad (14)$$

subject to the constraints

$$\begin{aligned} \sum_j \alpha_j &= 0 \\ \text{Im}(\hat{z}_N(\boldsymbol{\alpha}_j)) &= \hat{y}_N = 0. \end{aligned} \quad (15)$$

A similar approach can be employed to define an optimization problem with respect to the area. It makes physical sense to pose a minimization problem with respect to the transport rate. Therefore, we minimize w_N given the cross-sectional area of the pipe. In view of equation (13) the problem is formulated as follows:

$$\underset{\boldsymbol{\alpha}}{\text{maximize}} \quad \sum_{j=0}^{N-1} (\hat{y}_{j+1} + \hat{y}_j)(\hat{x}_{j+1} - \hat{x}_j) \quad (16)$$

subject to the constraints

$$\begin{aligned} \sum_j \alpha_j &= 0 \\ \text{Im}(\hat{z}_N(\boldsymbol{\alpha}_j)) &= \hat{y}_N = 0. \end{aligned} \quad (17)$$

The geometrical constraints (15) and (17) are necessary in view of the specific problem we are addressing (see Figures 1 and 2). Here, for ready reference, we clarify the parameters appearing in equation (11):

- The value of R is calculated through equation (4).
- As we have mentioned earlier, the Shape Optimization problem is an inverse problem. The classical approach is to compute the w_j s and R (with the exception of w_0) as the angles α_j s are known for a given shape. Here however, we need to compute the shape, hence we need to compute the angles α_j s and R , while the w_j s can be defined a priori without loss of generality, i.e. equispaced points between 0 and w_N .
- There is no explicit function for the objective function w_N . Its value is required a priori in the evaluation of \hat{z} (equation 11). Through application of the chain rule it can be easily justified that we can assume a value for w_N and the optimization procedure now provides the value of the dimensionless perimeter length (P), in the case of maximizing the transport rate, or the dimensionless area (A), in the case of minimizing the transport rate, through equations (12) and (13) respectively. This procedure suggests that maximizing the transport rate given the perimeter length of the pipe is equivalent to minimizing the length given the transport rate. Conversely, minimizing the transport rate given the cross sectional area of the pipe is equivalent to maximizing the area given the transport rate.

In the next section we solve numerically the two optimization problems, (14) and (16).

4.1 Model calculations

The Shape Optimization problems (14) and (16) are multidimensional, constrained, nonlinear, optimization problems. The objective is to find an efficient and versatile method to obtain the constrained maximum/minimum of the scalar function w_N with respect to the variables α_j that can be easily extended to a large number of variables and can handle complicated geometrical constraints. In view of the large number of variables and the complicated form of the objective function and constraints, we employ a numerical optimization method as outlined in [22] (it is a sequential programming method, where an estimate of the hessian of the lagrangian is updated at each iteration using the BFGS formula [10, 14]).

In order to evaluate the objective function and the nonlinear constraints it is required to compute the integral \hat{z}_i which has integrable power-law singularities when $\alpha_j < 0$. This is achieved through Gauss-Jacobi quadrature as outlined by Driscoll & Trefethen [8, 9]. Furthermore, we choose the \hat{w}_j s to be equispaced between 0 and 1 except near large slopes, i.e. when the α_j s are large, where we include some extra points in order to improve the accuracy.

In Figure (5) we show the optimal curves obtained from the numerical solution of the transport minimization problem (Shape Optimization problem 16). Four different cases are investigated, $w_N = 0.1, 1, 5$ and 10 , which correspond to Figures (a,b,c,d), respectively. The solid points correspond to the z_j s obtained through numerical optimization while the solid curves represent the analytical solution of the optimal shape obtained by Kacimov [19]:

$$x = \frac{1}{2\pi} \left(\ln \frac{m + \cos \theta}{m - \cos \theta} + \ln \frac{m + 1}{m - 1} \right), \quad y = \frac{1}{\pi} \arctan \frac{\sin \theta}{\sqrt{m^2 - 1}} \quad (18)$$

where $0 \leq \theta \leq \pi$. In the above equations:

$$m = \frac{\exp(\pi A)}{\sqrt{\exp(2\pi A) - 1}}$$

and A is the area (equation 13), obtained through

$$A = \frac{w_N^2}{2} \times (\text{maximum of the objective function}).$$

There is excellent agreement between the numerical results and the analytical solution. It is interesting to note that for large values of w_N ($w_N=5,10$; Figures 5c,5d) the optimal shapes do not exceed 0.5, i.e. one half the thickness of the slab [23].

In Figure (6) we show the optimal curves obtained from the numerical solution of the transport maximization problem (Shape Optimization problem 14). Similar to Figure (5) we have used the values $w_N = 0.1, 1, 5$ and 10 , which correspond to Figures (a,b,c,d), respectively. The solid points correspond to the z_j s obtained through numerical optimization while, motivated by the previous problem, the solid curves represent a curve-fit to the parametric equations

$$x = \frac{a}{2\pi} \left(\ln \frac{m + \cos \theta}{m - \cos \theta} + \ln \frac{m + 1}{m - 1} \right), \quad y = \frac{2}{\pi} \arctan \frac{\sin \theta}{\sqrt{m^2 - 1}}, \quad (19)$$

by choosing appropriate values for m and a . For small values of w_N ($w_N=0.1$; Figure 6a), i.e. small transport rates, we obtain that the circle (cylinder) is the optimal shape in agreement with the transport minimization problem. The agreement is not surprising in view of the isoperimetric theorem [24]. As the values of w_N increases the optimal shapes become elliptical ($w_N=1$; Figure 6b), while for large values of w_N ($w_N=5,10$; Figures 6c, 6d) the optimal shapes become rectangular and spike-like approaching the upper surface of the slab.

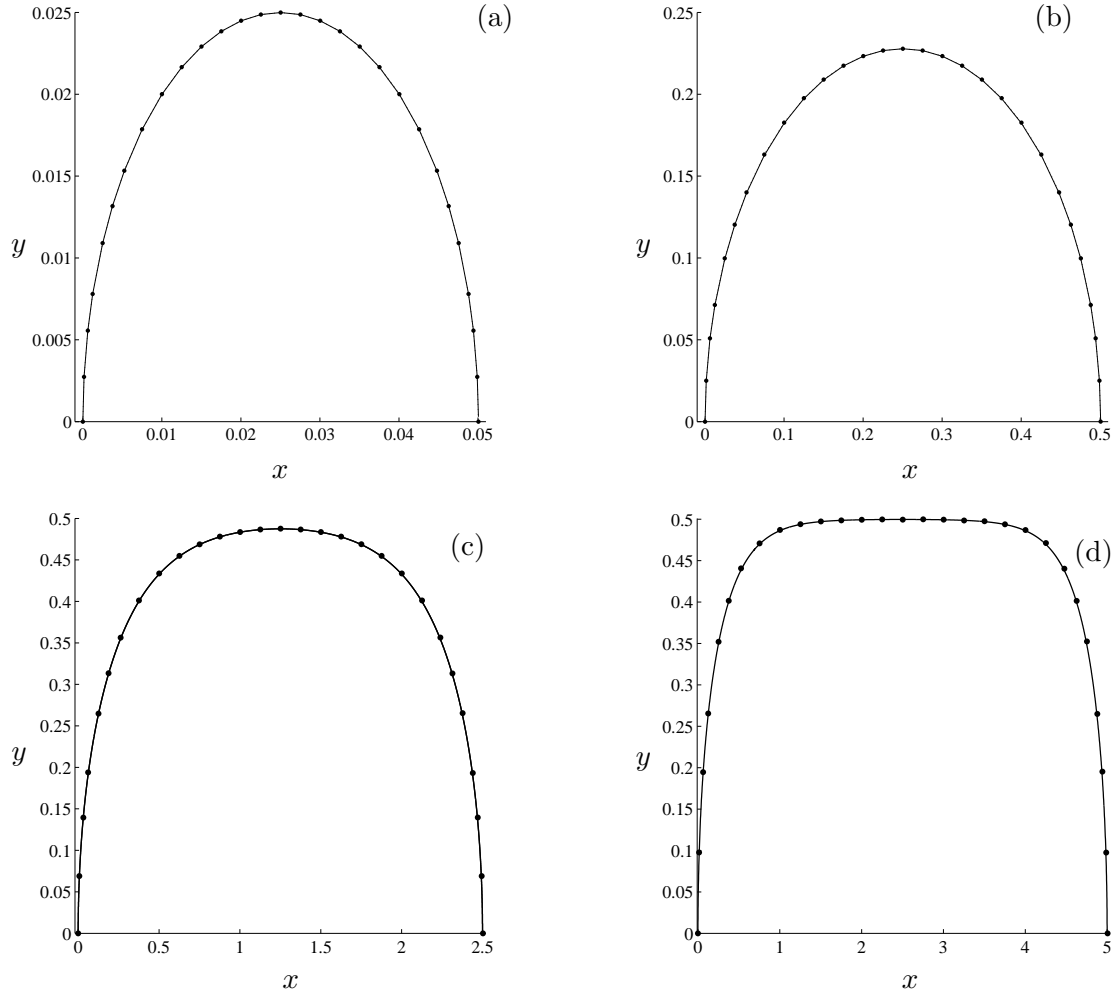


Figure 5: Optimal curves associated with minimizing the transport rate. In the figures we show results for $w_N = 0.1, 1, 5$ and 10 which correspond to Figures a,b,c and d respectively. The points correspond to the numerical results while the solid curves to the analytical results, i.e. parametric equations (18).

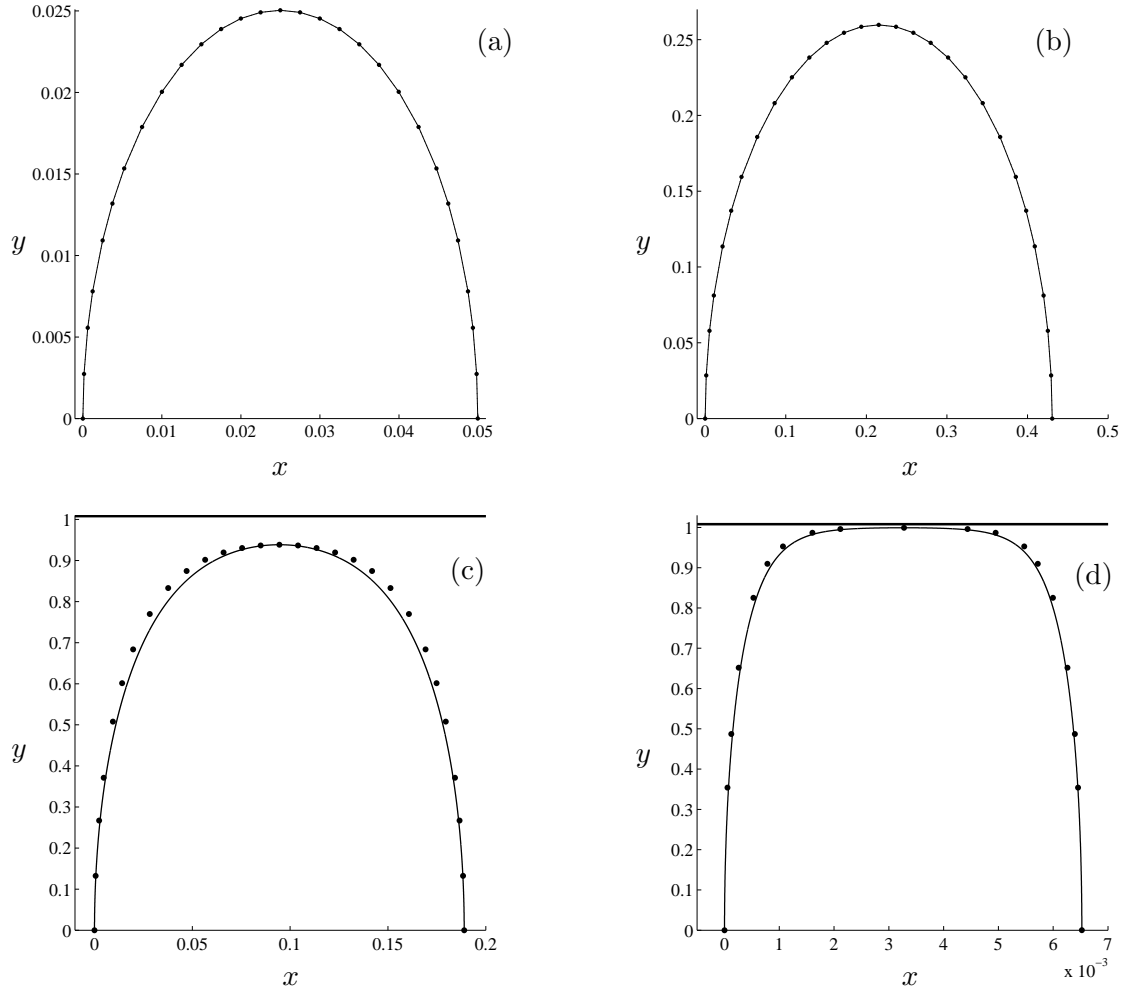


Figure 6: Optimal curves associated with maximizing the transport rate. In the figures we show results for $w_N = 0.1, 1, 5$ and 10 which correspond to Figures a,b,c and d respectively. The points correspond to the numerical results while the solid curves represent the parametric equations (19) by choosing appropriate values for m and a .

5 Conclusions

We have addressed the problem of heat conduction in a slab whose upper and lower surfaces are kept at a constant temperature. At the center of the slab there is a two-dimensional, isothermal, symmetric pipe. The problem (Laplace equation) is addressed using conformal mapping techniques (the generalized Schwarz-Christoffel transformation) where the two-

dimensional pipe, of general cross section, is mapped into a strip. The strip problem is solved using Fourier transform techniques to obtain a Fredholm integral equation of the first kind for the temperature gradient along the strip. The integral equation is addressed both analytically and numerically with excellent agreement between the analytical/asymptotic and numerical results. The Shape Factor of the pipe is equal to the Shape Factor of the strip.

The fact that the Shape Factor is a monotonic function of the length of the strip suggests using the length of the strip as the objective function in an optimization procedure where the variables of the optimization are the parameters of the generalized Schwarz-Christoffel transformation. We address two Shape Optimization problems associated with maximizing or minimizing the transport rate from a two-dimensional pipe of unit span: i) for a given surface area, obtain the shape of the pipe that maximizes the transport rate, ii) for a given volume, obtain the shape of the pipe that minimizes the transport rate. Equivalently, the Shape Optimization problems can be formulated as follows: i) given the transport rate, obtain the shape of the pipe that minimizes the perimeter length and ii) given the transport rate, obtain the shape of the pipe that maximizes the cross-sectional area. Optimal shapes for the problem of minimizing the conduction rate are computed numerically and validated with an analytical solution. Numerical results for maximizing the transport rate are also obtained. The versatility and the robustness of the numerical optimization algorithm offers opportunities for improving the design of such processes.

A Appendix: Useful Integrals

For $0 \leq \hat{\xi} \leq 1$ we have

$$\int_0^1 \frac{\ln(|\hat{\xi} - \hat{\theta}|)}{\sqrt{\hat{\theta}(1-\hat{\theta})}} d\hat{\theta} = -\pi \ln(4) \quad (20)$$

The integral can be obtained by an appropriate change of variables in the integrals listed in [21].

The inverse Fourier transform of $\tanh w/w$ is defined as [20]

$$\frac{1}{\sqrt{2\pi}} \int_{-\infty}^{\infty} \frac{\tanh w}{w} e^{iw\xi} dw = \frac{1}{\sqrt{2\pi}} \int_{-\infty}^{\infty} \frac{\tanh w}{w} (\cos(w\xi) + i \sin(w\xi)) dw,$$

and simplifies to

$$\frac{1}{\sqrt{2\pi}} \int_{-\infty}^{\infty} \frac{\tanh w}{w} e^{iw\xi} dw = \frac{2}{\sqrt{2\pi}} \int_0^{\infty} \frac{\tanh w}{w} \cos(w\xi) dw,$$

because $\tanh w/w$ is an even function. In view of the following integral listed in [1]:

$$\int_0^{\infty} \frac{\tanh w}{w} \cos(w\xi) dw = \log \left[\coth \left(\frac{\pi\xi}{4} \right) \right],$$

the Fourier transform simplifies to

$$\frac{1}{\sqrt{2\pi}} \int_{-\infty}^{\infty} \frac{\tanh w}{w} e^{iw\xi} dw = \sqrt{\frac{2}{\pi}} \log \left[\coth \left(\frac{\pi|\xi|}{4} \right) \right]. \quad (21)$$

References

- [1] H. Bateman, *Tables of Integral Transforms* (McGraw-Hill Book Company, Inc, 1954).
- [2] A. Bejan, *Shape and Structure, from Engineering to Nature* (Cambridge University Press, Cambridge, UK, 2000).
- [3] C. Biserni, L. A. O. Rocha & A. Bejan, Inverted fins: geometric optimization of the intrusion into a conducting wall, *Int. J. Heat Mass Transfer* **47**, 2577 (2004).
- [4] H. S. Carslaw & J. C. Jaeger, *Conduction of heat in solids* (Clarendon Press, 1959).
- [5] K. S. Choi & K. K. Prasad & T. V. Truong, *Emerging Techniques in Drag Reduction* (Mechanical Eng. Publ., London, 1996).
- [6] R. T. Davis, Numerical methods for coordinate generation based on Schwarz-Christoffel transformation, AIAA Paper No. 79-1463, 4th Computational Fluid Dynamics Conference 180 (1979).
- [7] G. De Mey, Temperature distribution in floor heating systems, *Int. J. Heat Mass Transfer* **23**, 1289 (1980).
- [8] T. A. Driscoll & L. N. Trefethen, *Schwarz-Christoffel Mapping* (Cambridge University Press, 2002).
- [9] T. A. Driscoll, *Schwarz-Christoffel Toolbox Users Guide*.
- [10] R. Fletcher & M. J. D. Powell, A rapidly convergent descent method for minimization, *Computer Journal* **6**, 163 (1963).
- [11] R. Fletcher, *Practical Methods of Optimization* (John Wiley and Sons, 1987).
- [12] J. M. Floryan, Conformal-mapping-based coordinate generation method for channel flows, *Journal of Computational Physics* **58**, 229 (1985).
- [13] M. M. Fyrillas, Advection-dispersion mass transport associated with a non-aqueous-phase liquid pool. *J. of Fluid Mech.* **413**, 49 (2000).

- [14] D. Goldfarb, A family of variable metric updates derived by variational means, *Mathematics of computing* **24**, 23 (1970).
- [15] E. Hahne & U. Grigull, Shape factor and shape resistance for steady multidimensional heat conduction. *Int. J. Heat Mass Transfer* **18**, 751 (1975).
- [16] D. Homentcovschi & L. Jude, Potential due to some arbitrary charged strips between parallel earthed planes. *Int. J. Engng Sci.* **22**, 775 (1984).
- [17] F. P. Incropera & D. P. DeWitt, *Fundamentals of Heat and Mass Transfer* (John Wiley & Sons, 1990).
- [18] A. R. Kacimov, Analytical solution and shape optimization for groundwater flow through a leaky porous trough subjacent to an aquifer. *Proc. R. Soc. Lond. A*, **462**, 1409 (2006).
- [19] A. Kacimov, Optimal shape of variable condenser. *Proc. R. Soc. Lond. A*, **457**, 485 (2001).
- [20] E. Kreyszig, *Advanced Engineering Mathematics* (John Wiley & Sons, 1988).
- [21] W. Magnus & F. Oberhettinger *Formulas and theorems for the functions of mathematical physics* (Chelsea Publishing Company, New York, 1949).
- [22] *Optimization Toolbox*, The MathWorks Inc., 2000.
- [23] P. M. Morse & H. Feshbach *Methods of Theoretical Physics, Part II*, McGraw-Hill Science/Engineering/Math, 1953.
- [24] R. Osserman, *A Survey of Minimal Surfaces* (New York: Dover, 1986).
- [25] P. Payvar, Analytical solution of a new mixed boundary-value problem in heat conduction, *Q. Jl Mech. Appl. Math.* **32**, 253 (1979).
- [26] O. Pironneau, *Optimal shape design for elliptic systems* (Springer, New York, 1984).
- [27] K. B. Ranger, The solution of a new mixed boundary value problem by use of an integral transformation, *Int. J. Engng Sci.* **12**, 853 (1974).
- [28] S. S. Sadhal, Explicit solutions to a class of mixed boundary value problems, *Int. J. Engng Sci.* **19**, 1053 (1981).
- [29] H. A. Stone, Heat/mass transfer from surface films to shear flows at arbitrary Peclet numbers, *Phys. Fluids A* **1**, 1112 (1989).
- [30] P. K. Swamee, G. C. Mishra & B. R. Chahar, Design of minimum seepage loss canal sections with drainage layer at Shallow depth, *J. Irrig. and Drain. Engrg., ASCE*, **127**, 287 (2001).